Journal of Structural Geology, Vol. 10, No. 8, pp. 829 to 845, 1988
Printed in Great Britain

0191-8141/88 $03.00 + 0.00

Mechanisms of thrust propagation: some examples and implications for the analysis of overthrust terranes

PETER A. GEISER

Department of Geology and Geophysics, University of Connecticut, Storrs, CT 06268, U.S.A.

(*Received* 25 *February* 1986; *accepted in revised form* 2 *May* 1988)

Abstract—Evidence is presented for the existence of three fundamental mechanisms by which thrust sheets move. The mechanisms are: (1) failure of a stiff layer, to form ramp–flat geometry ('imbricated' thrust sheets); (2) detachment of a layer by folding ('décollement' thrust sheets); (3) differential layer-parallel shortening ('LPS' thrust sheets). The mechanisms are independent but may operate interactively to form families of 'hybrid' thrust sheets. Since LPS thrust sheets have not been previously described or documented, data from the New York plateau, deformed almost exclusively by differential LPS, is presented to demonstrate the physical characteristics of this thrust mechanism.

Information from the plateau indicates that finite-strain behavior closely reflects the geometric boundary conditions and is independent of temperature and depth of burial. Finite-strain data are used to construct a set of iso-strain maps in both the deformed and undeformed states. The iso-strain maps are in turn used to determine the displacement field for the thrust sheet. The displacement field allows visualization of the effects of both Lagrangian and Eulerian transformations on an initially orthogonal grid.

Utilizing sections from a number of overthrust belts, it is shown that the three mechanisms occur universally although in various proportions. LPS is regionally developed throughout the central and northern Appalachians. The presence of the LPS thrust sheets probably accounts for the failure of structural cross-sections to bed-length balance in these blind thrust terranes. Finally a series of examples drawn from the field as well as the literature are used to illustrate both the characteristics of hybrid thrust sheet families as well as to indicate how knowledge of their behavior can be utilized in developing strategies for the construction and balancing of structural cross-sections.

INTRODUCTION

BOYER & Elliott (1982) have proposed that the term 'thrust sheet' be applied to any body of rock bounded below by a thrust fault. The motion of the thrust sheet is accommodated by the strain within the sheet. This strain is a combination of rigid-body translation, internal rotations (folding) and distortions (layer-parallel shortening, LPS) and represents the set of mechanisms by which thrust sheet motion occurs. The present concept of a thrust sheet is strongly associated with the original 'stair case' trajectory described by Rich (1934). The motion and geometry of thrust sheets of this type are primarily the product of rigid-body translation with minor internal bending strains as the sheet moves over the ramp–flat structure of the fault surface (e.g. Suppe 1983). In theory it is possible to have thrust sheet motion accommodated by any of the three types of strain, either singly or in combination.

The purpose of this paper is the following:

(i) to demonstrate that the proportion of rigid-body translation to various types of internal strain of the sheet is not restricted to that represented by the type of analysis given by Suppe (1983), in which internal distortion is minimal and restricted to that produced by flexural flow. Instead the proportion of rigid-body translation to other strains accommodating thrust sheet motion represents a broad spectrum of variation, bounded by three end-members ranging from thrust sheets with zero or minimal LPS and folding to thrust sheets dominated by either folding or LPS (Fig. 1);

(ii) to point out that since the thrust tip is a part of the thrust sheet, the three mechanisms are also the means by which tip propagation occurs;

(iii) to show that by thinking in terms of the kinematics of thrust sheet and thrust system motion and its accommodation by finite strain, the notion of the interplay of the three end-members and the resulting hybrid thrust sheets can be of material aid in the construction and balancing of geological cross-sections;

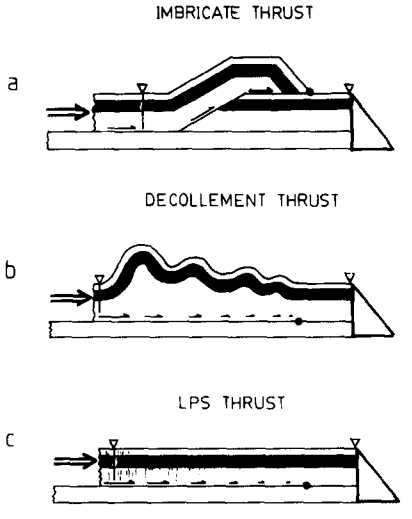

Fig. 1. Mechanisms of thrust sheet motion: (a) shortening of thrust sheet by doubling of stiff layer by *imbrication*; (b) shortening of thrust sheet by folding and development of *décollement*; (c) shortening of thrust sheet by differential *LPS* between ductile upper layer and more rigid substrate.

(iv) since thrust sheets whose motion is accommodated primarily by LPS have not previously been described, the bulk of the paper is concerned with documenting the existence, nature and geometry of these structures.

The term 'stiff layer' is used to describe those units which form ramps and become imbricated while the term 'roof layer' describes the units structurally above the stiff layer and separated from it by a roof thrust. The roof thrust concept of Boyer & Elliott (1982) is generalized to designate the zone along which differential motion between the imbricated layer and the overlying roof layer is concentrated.

Figure 1 shows the three end-member mechanisms of thrust sheet motion. These are: (1) motion resulting from the failure of a 'stiff layer', thereby allowing the sheet to move over itself (Fig. 1a); (2) folding of a ductile layer above an underlying undeformed less ductile layer (Fig. 1b); (3) differential LPS between a ductile hanging-wall and a more rigid footwall (Fig. 1c). To retain clarity and carry through the idea of the three different mechanisms, I will use the term *imbricate* for motions of the first type, *décollement* for the second and *LPS* for the third. Thrust sheets formed by the first mechanism are termed *imbricate thrust sheets*, those formed by the second mechanism *décollement thrust sheets* and those formed by the third mechanism *LPS thrust sheets*.

Blind thrusting and the case for layer shortening thrusts

Numerous cases of blind thrusting have been documented in the central Appalachians (Gwinn 1964, 1970, Perry 1978), yet the geometric problem of accounting for the displacement on these thrusts is lightly treated. An exception is Thompson (1979), who implicitly recognized that in order for a blind horse to move without significant imbrication of the displaced roof layer, some alternative method of accommodating the roof layer is required. Thompson described the accommodation of inserting the stiff layer into its roof layer as a back-directed décollement thrust sheet developed over the top of a forelimb and a forward-directed décollement thrust sheet in front of the forelimb (Fig. 2). As described, the two types of thrust sheet are kinematically linked to form a hybrid, two-tiered system, a lower imbricate thrust sheet and an upper décollement thrust sheet. Kulander & Dean (1986) have described a similar system in the southern part of the central Appalachian Valley and Ridge, explicitly referring to the stiff layer and the more ductile roof layer as separate thrust sheets.

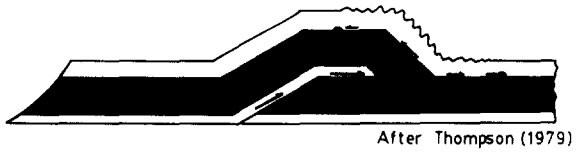

Fig. 2. Schematic illustration of hybrid thrust sheet formed by imbrication and décollement. Filled circles indicate fault tips.

The critical point is that in a blind thrust terrane, the displacement of the stiff layer must be accommodated by some mechanism in the roof layer (a kinematically admissible section, Fig. 3 and Geiser 1988a,b), since the roof layer material must have a means of moving out of the way of the thrust sheet being inserted, otherwise the section is not physically possible (a kinematically inadmissible section, Fig. 3).

In the central and northern Appalachians, where the subsurface is dominated by blind imbrication, it is not possible to bed-length balance the stiff layer and roof layer (see Gwinn 1964, 1970, Wiltschko & Chapple 1977, Perry 1978, Herman 1984 and Fig. 4 for examples). Recognizing the problem, Perry (1978) proposed that the displacement of the roof layer was absorbed on the plateau. However the shortening due to folding and thrusting on the plateau is only of the order of 2–5% of the total displacement of the roof layer which must be accounted for (see, for example, Gwinn 1964, 1970 and state geologic maps of Pennsylvania, West Virginia and New York). This discrepancy can be explained by examining the relationship between LPS and detachment in the New York plateau.

DEFORMATION IN THE NEW YORK PLATEAU

Relationship between mesoscopic fabric elements and detachment

Beginning with Nickelsen (1966), a body of knowledge has accumulated on the LPS strain in the Appalachian plateau and Valley and Ridge of New York and Pennsylvania (Engelder & Engelder 1977, Engelder & Geiser 1979, 1980, Geiser & Engelder 1983). An important aspect of this work is the recognition of a regionally-developed set of fabric elements (fossil distortion, spaced solution cleavage, penciling and crenulations) associated with LPS and predating finite-amplitude folding (Geiser 1970, 1974, Faill & Nickelsen 1973, Engelder & Geiser 1979). Geiser & Engelder (1983) use the term 'LPS fabric' for this set of structures.

A striking aspect of the LPS fabric is seen on the New York plateau, where a direct correspondence exists between the distributions of salt, located in the Middle Silurian Salina group, and the LPS fabric: the LPS fabric is only found in the region occupied by the salt and essentially ends at the zero isopach (Fig. 5). East of the salt pinch-out, lithologies sensitive to LPS effects show none (Slaughter 1982). As the salt is a known detachment horizon in both the Pennsylvania and New York plateaus (Gwinn 1964, 1970, Rodgers 1970, Wiltschko & Chapple 1977), this demonstrates a clear correlation between the LPS fabric and detachment.

Relationship between finite strain and detachment

Bulk finite strain in the plateau is partitioned among as many as five mechanisms: (1) intragranular deformation; (2) pressure solution; (3) folding; (4) extension

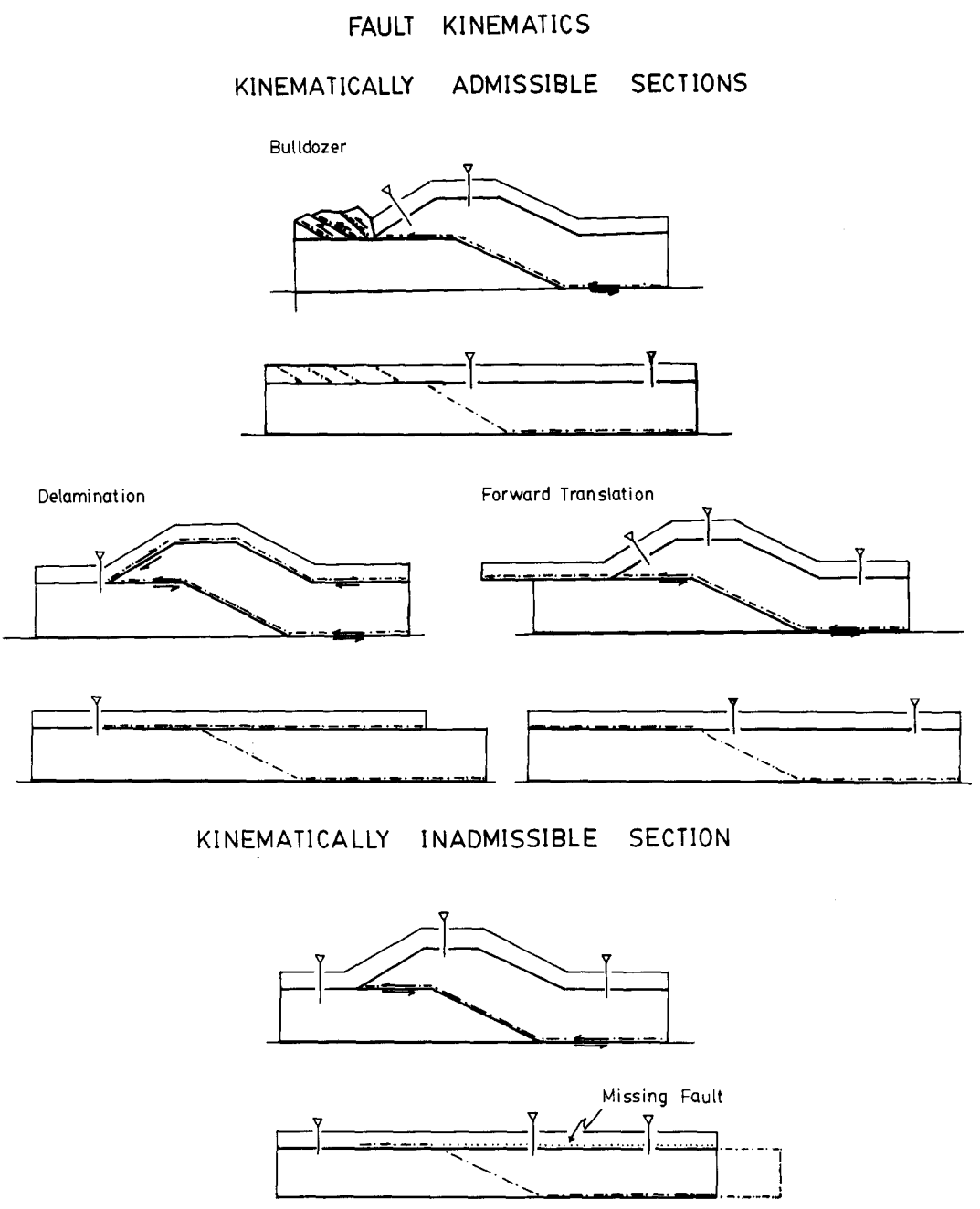

Fig. 3. Schematic diagram showing kinematically admissible solutions for thrust faults in blind thrust terranes. Except for 'delamination', transfer of displacement from base of stiff layer to base of the roof layer produces significant deformation of the roof layer. Note that there are three different possible solutions for the same superficially similar sections (from Geiser 1988b).

cracking; and probably (5) grain-boundary sliding. New York plateau LPS data is principally derived from study of the abundant crinoid columnals present in all the units of the Devonian Catskill delta. Details are given by Engelder & Engelder (1977), Engelder (1979a,b), Engelder & Geiser (1979) and Slaughter (1982). Strains derived from these deformed fossils are shown relative to the Silurian salt isopachs (Fig. 5).

To explore the relationship between LPS and the detachment in more detail, five strain profiles through the data set have been constructed (Fig. 6). Three of the profiles (AA', DD', EE') end at the zero salt isopach. The profile locations were selected on the basis of density of data (Fig. 5). Folding strain was determined using Wedel's (1932) structure contour map. Limb dips on these folds are 2° or less with structural relief 180 m or less. The total sinuous bed-length shortening of these folds gives a strain of $(1 + e) = 0.9999$. The remainder of the bulk finite strain is due to LPS.

As Engelder (1979a) shows, the shape change of the columnals, actually reflects a partitioning of the strain between two mechanisms, pressure solution and mechanical twinning. The importance of grain size in determining mechanical behavior (Elliott 1973) suggests that the large relative grain size of the crinoid ossicles may make them stronger than their silt and clay size matrix. Thus the strain recorded by the crinoid columnals is probably a minimum.

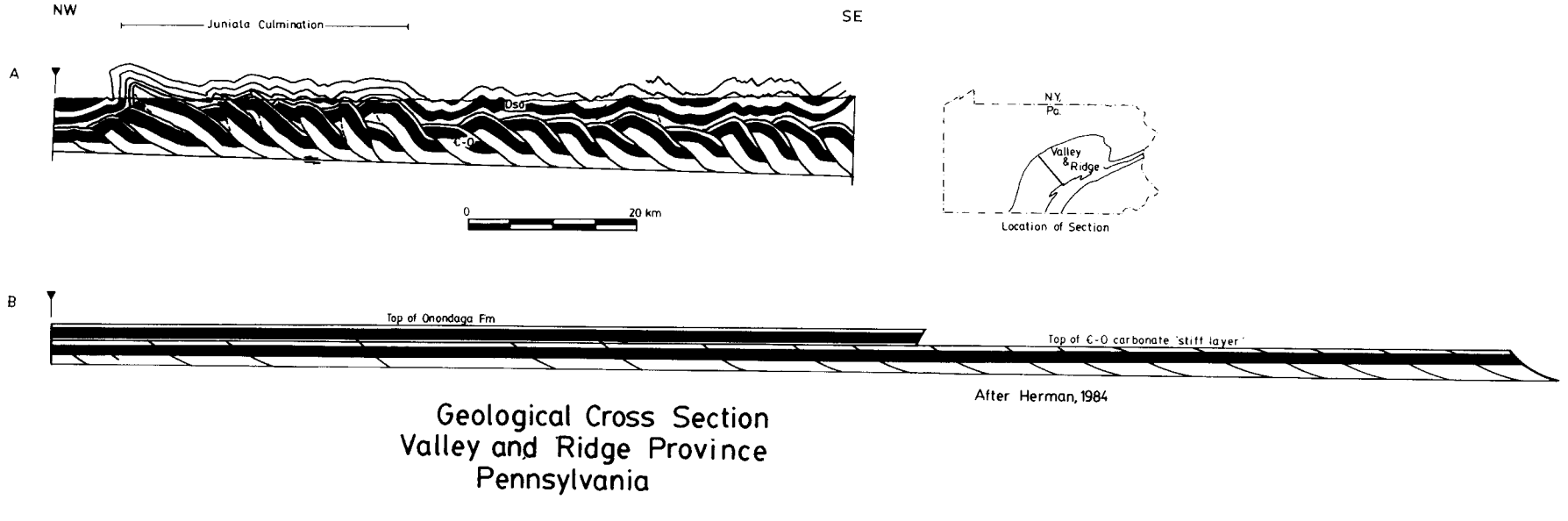

Fig. 4. Balanced (i.e. restorable and admissible) section through the Juniata Culmination demonstrating difference in bed-length between roof layer and stiff layer characteristic of much of the central and northern Appalachian Valley and Ridge province (from Herman 1984). (a) The deformed-state section showing the fault array. (b) The undeformed-state section showing the fracture array. C–O, Cambrian–Ordovician; DSO, Devonian–Silurian.

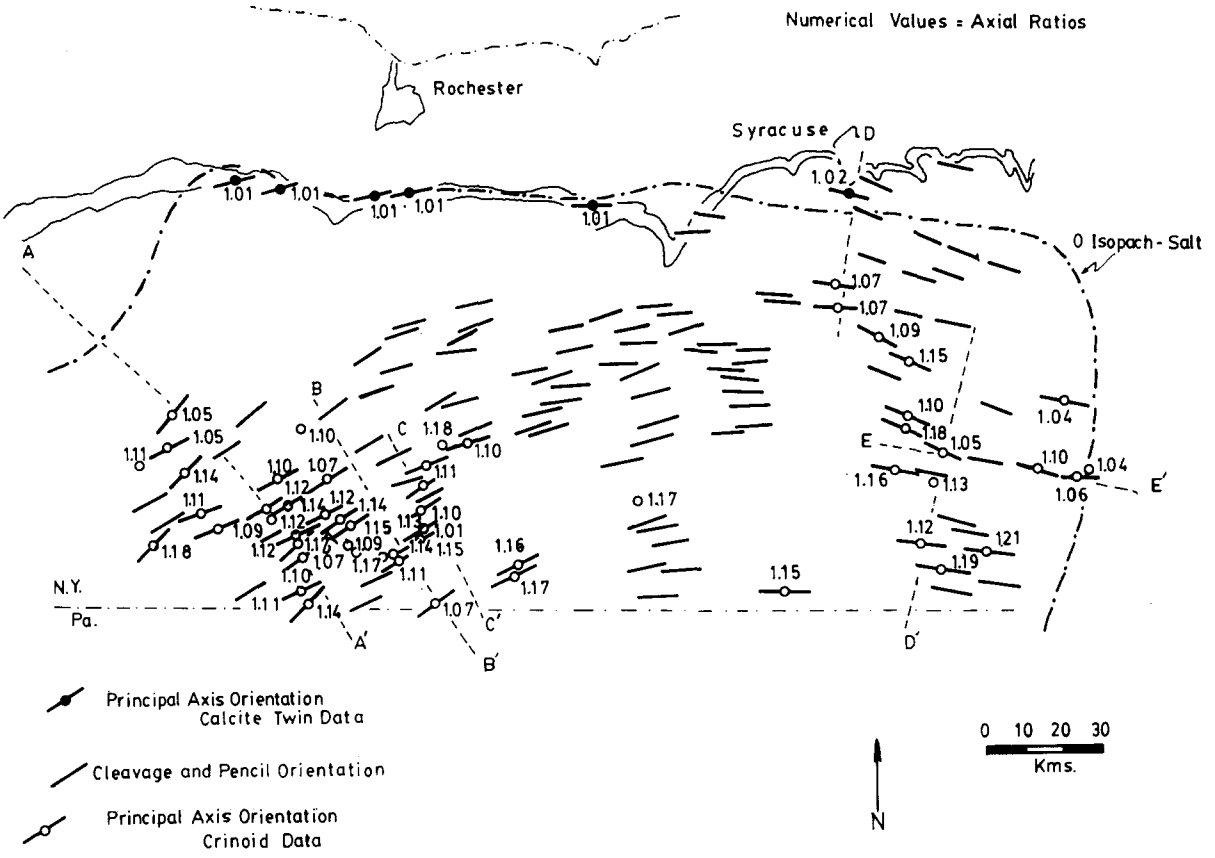

Fig. 5. Finite-strain data set for the New York plateau (from Geiser 1988b). Data from Engelder (1979a), Engelder & Geiser (1980) and Slaughter (1982).

There is a significant difference in the variability of the axial ratios of the crinoid ossicles between the eastern and western profile lines. The eastern lines (DD′ and EE′, Fig. 5), with low sampling density, show a good correlation (r = 0.879 and 0.958, respectively; Fig. 6a) with a linear strain gradient. The western lines (AA′, BB′ and CC′, Fig. 5), with a more dense sampling, show a poorer fit to a linear strain gradient (r = 0.696, 0.224 and 0.902, respectively, Fig. 6b). It is unclear whether this is due to greater strain heterogeneity in the west or to the contrast in density of data between east and west. For the purpose of calculation I have assumed that the gradient along any finite-strain trajectory is linear.

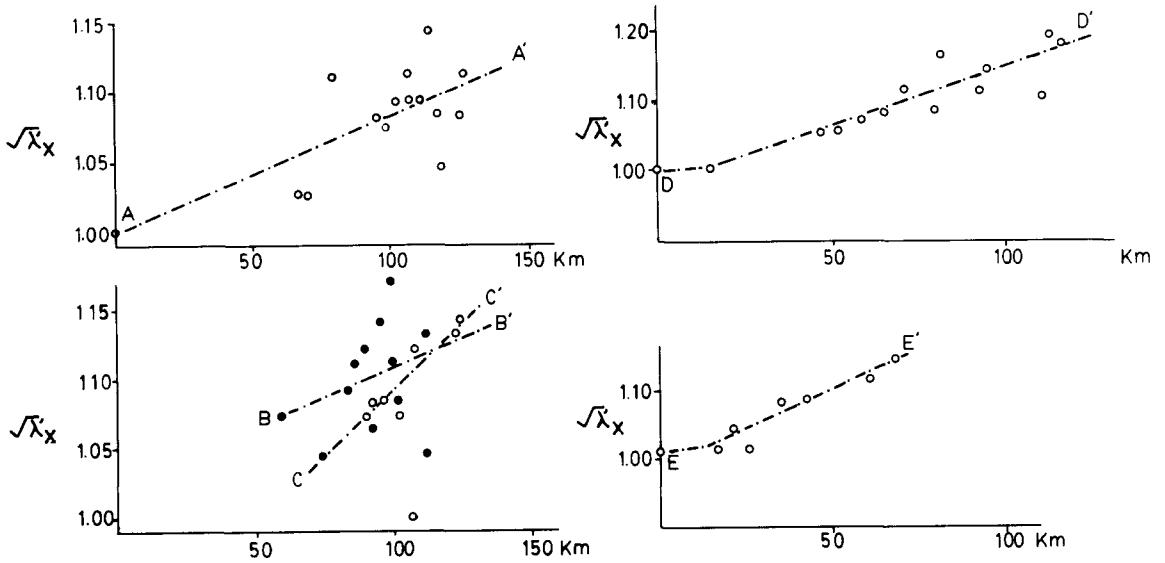

Fig. 6. Plots of axial ratio (a/c) vs distance for the profiles shown in Fig. 5. Bulk strain values shown in Fig. 5 were recalculated using equation (6) with corrected values for calcite twin strain.

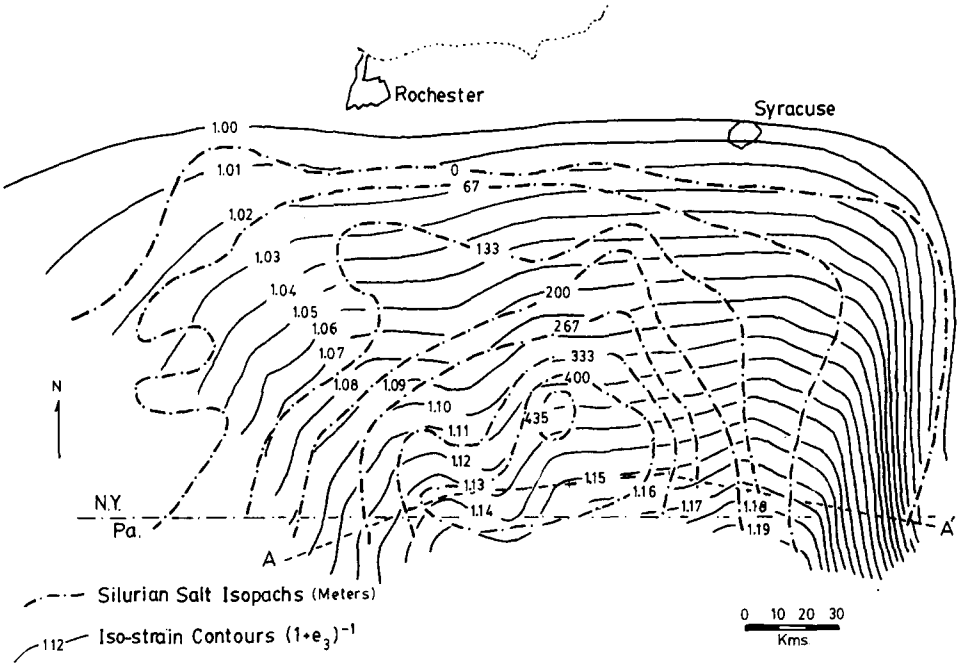

Fig. 7. Relationship between the iso-strain contours and Silurian salt isopachs (from Geiser 1988b).

Determination of finite-strain values, New York plateau

This section describes the method by which finite-strain values were calculated from the axial ratios of the crinoid ossicles and calcite twin data. The goal is to define the strain as completely as possible by determining the displacement field for the New York plateau. The data set for this region has the following limitations with regard to these calculations: (1) the strain recorded by the columnals may only be a minimum; (2) direct evidence on the orientation and magnitude of the bulk finite-strain ellipse (FSE) consists of measurements of the *a/c* (long axis/short axis) ratios of the columnals in the plane of the bedding, calcite mechanical twin strain data and the orientation of cleavage and pencils; (3) the cleavage orientation is consistently normal to bedding, suggesting that bedding is a principal plane of the FSE for pressure solution mechanisms. However, the calcite twin data (Table 1) indicates that bedding is a general section through the twin strain FSE; (4) Slaughter's (1982) work demonstrates that, at least locally, strain partitioning in the crinoid columnals differs between the eastern and western parts of the plateau. In the western part, pressure solution is the dominant mechanism, while in the east what may be a previously unrecognized dislocation–creep mechanism sometimes dominates. Evidence for this is given by angular changes between crenulae within the crinoid columnals, a phenomenon only observed in the eastern part of the New York plateau where Conodont Alteration Indices (CAI) suggest higher temperatures may have occurred. Calculations of the strain required to produce the observed angular changes is consistent with the measured aspect ratios, but much larger than the strains indicated by the observable calcite twins (Slaughter 1982).

The deformation of an initially orthogonal grid is a good visual representation of strain geometry. Creation of such an image requires that the displacement field be known. In general the displacement field cannot be determined from the finite strain (see Ramsay & Huber 1983) except in the case of uniform area strain (Cutler & Elliott 1983). Fortunately the state of strain of the New York plateau very closely approximates this case (Geiser 1988b) permitting the direction of the displacement vectors to be determined from the orientation of the various LPS fabric elements (Cutler & Elliott 1983).

The magnitudes of the displacement vectors can be determined by the use of the deformed-state iso-strain contours (Fig. 7) prepared from the finite-strain data shown in Fig. 5. The strain integration techniques outlined by Ramsay (1969) and Hossack (1978) allow either the deformed- or undeformed-state positions of material lines to be located along principal strain trajectories. These techniques allow transformation of material lines from the deformed to undeformed states. Thus strain integration along the finite-strain trajectories allows location of the iso-strain contours in the undeformed state. The method is shown schematically in Fig. 8.

As discussed by Ramsay (1969) and Hossack (1978) the equation for the calculation involves a simple integral of the type $L_0 = \int \sqrt{\lambda} dl$, where $\lambda = f(l)$. To transform from the undeformed state to the deformed state we use $\lambda = f(l)$ and to transform from the deformed to the undeformed states we use $\lambda' = f(l')$.

The crinoid data demonstrate that solution effects are highly anisotropic, acting primarily on surfaces normal to the maximum compressive stress direction (Engelder 1979a,b). Consequently the crinoid data reflects LPS strain rather than an isotropic volume loss, thus the

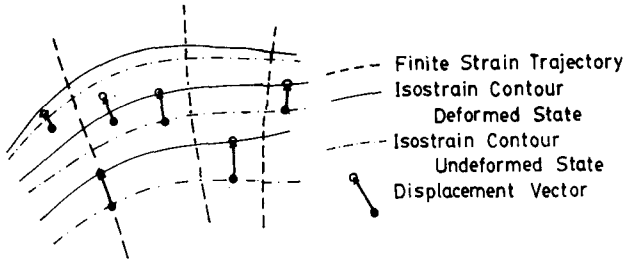

Fig. 8. Schematic illustration of the method of displacement-field construction from finite-strain data for uniform area strain. Directions of vectors are given by principal directions derived from LPS fabrics; magnitudes of vectors are given by the difference beween iso-strain contours in the deformed and undeformed states (from Geiser 1988b).

equations derived by Hossack (1978) are used rather than those of Ramsay (1969).

To develop an expression for the function $\sqrt{\lambda'}$, consider a columnal lying with its [0001] axis normal to the bedding. This gives an initially circular section of unit radius, deformed into an ellipse by a combination of both pressure solution and intragranular mechanisms. Let a and c, respectively, be the major and minor semi-axes of this ellipse. To find an expression for the changes in length of the lines that become the ellipse axes, choose a co-ordinate frame with x parallel to c and y parallel to a. For a line parallel to x:

$$c = 1 + \Delta x_p + \Delta x_i \tag{1a}$$

and for a line parallel to y

$$a = 1 + \Delta y_p + \Delta y_i, \tag{1b}$$

where Δx_p = change in length due to pressure solution and Δx_i = change in length due to intragranular strain, with the same meaning applied to the set of prefixes associated with the y values. The strain of the crinoid columnal in terms of the *reciprocal* quadratic elongation λ' is expressed as

$$a/c = \sqrt{\lambda'_x}/\sqrt{\lambda'_y} = m \tag{2}$$

$$\sqrt{\lambda'_x} = m\sqrt{\lambda'_y}. \tag{3}$$

Data on the bulk FSE is given by the crinoid columnals in the form of the aspect ratio of the principal strains in the plane of the bedding, determined by the tensor strain average techniques of Shimamoto & Ikeda (1976).

Equation (3) is an expression for $\sqrt{\lambda'_x}$ in terms of the aspect ratio m and the finite strain in the y direction. This, substituted into the equation for the integrated strain (Hossack 1978), is the operator giving the undeformed length of a line. Thus to find the original length of any line parallel to a principal trajectory in the deformed state we have the following expression given in terms of the elongation e:

$$x_o = \int (m/(1 + e_y))\, dx. \tag{4}$$

As m is known we need only a value for e_y. By definition, $e_y = \Delta y$, where $\Delta y = \Delta y_p + \Delta y_i$. Because there is no solution–precipitation in the form of calcite 'beards' in the y direction (Engelder 1979a,b, Slaughter 1982) $\Delta y_p = 0$. Consequently

$$e_y = \Delta y_i. \tag{5}$$

Substituting equation (5) into equation (4) gives the final expression for calculating the initial length of a line parallel to a principal strain trajectory,

$$x_o = \int m/(1 + \Delta y_i)\, dx. \tag{6}$$

Although the plane of bedding is a principal plane for the finite strain due to pressure solution (Engelder 1979a,b, Engelder & Geiser 1979) it is not for the twin strain (see Table 1 and Engelder 1979a). The problem is significant with regard to the magnitude of the intragranular deformation in the plane of bedding (Δy_i) which is only a component of the total twin strain. The magnitude of this component can be found from the three-dimensional twin strain data by finding the general section of the twin strain ellipsoid parallel to the plane of bedding. The following equation relates the direction cosines (i, j, k) of the normal to a plane of section of a triaxial ellipsoid to the principal axes ($\lambda_1, \lambda_2, \lambda_3$):

$$[\lambda_1^2 i^2]/[n^2 - \lambda_1^2] + [\lambda_2^2 j^2]/[n^2 - \lambda_2^2] + [\lambda_3^2 k^2]/[n^2 - \lambda_3^2] = 0.$$

The roots n of this equation give the magnitudes of the principal axes, while bedding is the plane of interest for the case at hand. Substituting values for i, j, k and λ_1, λ_2, λ_3 from the calcite twin data of Engelder (1979a) and Slaughter (1982) gives the results shown in Table 1. These data show that for lines AA′, BB′ and CC′ the mean value for the component of twin strain in the plane of bedding is $\Delta y_i = +0.024$, while for the eastern line DD′, $\Delta y_i = +0.015$.

Values for $\sqrt{\lambda'_x}$ can be calculated using equation (3), where the mean calcite twin strain values, as determined

Table 1. Finite-strain data set, New York plateau

Location	A	B		C		D
		$\sqrt{\lambda_3}$	$\sqrt{\lambda_2}$	$\sqrt{\lambda_x}$	$\sqrt{\lambda_y}$	$\sqrt{\lambda_x}$
BRO 48	1.10	0.95	1.03	0.95	1.02	0.92
CHE 27	1.10	0.96	1.00	0.96	1.00	0.92
CHE 25	1.06	0.93	1.02	0.93	1.00	0.95
CHE 16	1.04	0.94	1.01	0.95	1.01	0.98
DEL 3	1.04	0.94	1.01	0.94	1.02	0.97
BRO 32	1.19	0.94	1.01	0.95	1.01	0.85
BRO 11	1.21	0.93	1.02	0.96	1.01	0.83
BRO 31	1.18	0.94	1.01	0.94	1.02	0.86
COR 10	1.10	0.95	1.03	0.95	1.03	0.92
COR 11	1.09	0.94	1.02	0.95	1.00	0.93
TRI	1.05	0.98	1.01	0.97	1.00	0.97
SMB	1.15	0.98	1.00	0.98	1.01	0.89
ADI	1.17	0.94	1.01	0.95	1.02	0.87
AND	1.15	0.94	1.05	0.95	1.02	0.89
VAN 1	1.18	0.98	1.04	1.00	1.03	0.867
CAM	—	0.92	1.05	0.93	1.02	—
RAW	1.13	—	—	—	—	—

A = Bulk finite strain ratio, $\sqrt{\lambda_y}/\sqrt{\lambda_x} = m$ (in plane of bedding).
B = Measured calcite twin strain (three-dimensional).
C = Calculated calcite twin strain in plane of bedding.
D = $(1 + e_3) = \lambda_x$ calculated in plane of bedding (for input into equation 6).

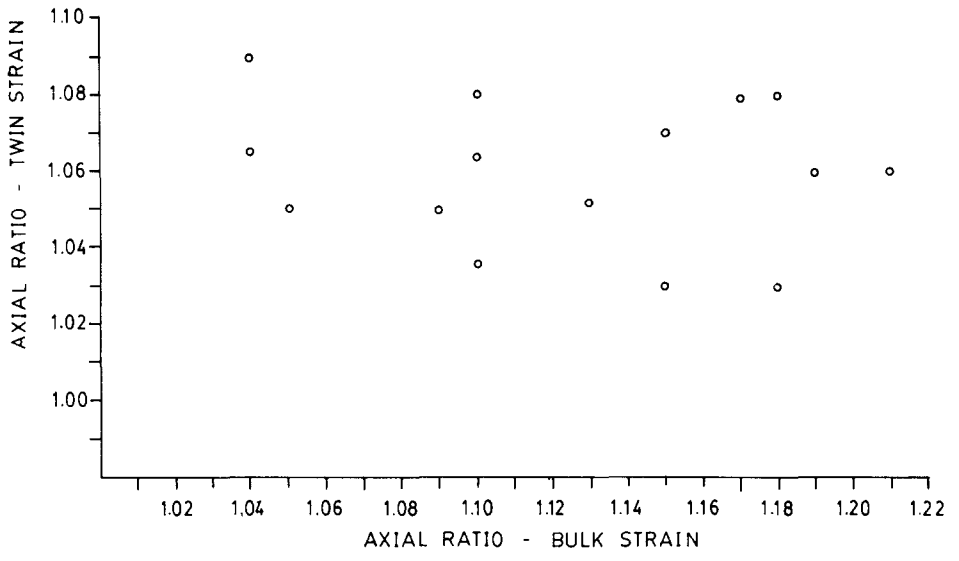

Fig. 9. Plot of twin strain axial ratio vs the axial ratio of bulk finite strain.

above, give the value of Δy_i, and the values of m are from the data set shown in Fig. 5. The results, given in Table 1, have been used to determine strain gradients along the finite-strain trajectories shown in Fig. 5. The mean slope for the area covered by lines AA', BB', and CC' is $\Delta\sqrt{\lambda_x'}/km = +0.0011$, while for line DD' it is $\Delta\sqrt{\lambda_x'}/km = +0.0016$ (Fig. 6a & b). Strain values can be found for any point in the region shown in Fig. 5, by assuming a linear gradient along both the λ_x and λ_y trajectories and interpolating between the data sets. The values found this way are used to construct the iso-strain map (Fig. 7).

Strain partitioning

Strain partitioning, as defined by Mitra (1978), requires knowledge of the complete three-dimensional strain. Unfortunately the calcite twin data alone gives such information, consequently only the relationship between the strain ratios of the various components in the plane of bedding can be found. Again only the calcite twin- and bulk-strain ratios can be determined independently. Plotting the two ratios against each other shows that the twin strain ratio is independent of the bulk strain (Fig. 9). As Table 1 and Slaughter (1982) show, the magnitude of the twin strain remains almost constant, while the bulk finite strain increases towards the regions of thicker salt. Thus the partitioning ratio for calcite twin strain must decrease towards the interior of the sheet away from the zero salt isopach.

Although it is true that for pressure solution $(1 + e_y) = 1.0$, this claim cannot be made for the additional intragranular component found by Slaughter (1982). Unfortunately the available data set does not contain sufficient information to independently determine these values, as separate measures of the pressure solution and intragranular strains have not been devised. At this time only a qualitative estimate can be made for the strain partitioning, and this is to simply note that the evidence shown by Engelder (1979a,b) and Slaughter (1982) suggests that the importance of pressure solution increases westward, while intragranular deformation mechanisms increase in significance eastward.

Discussion: finite strain in the New York plateau

The data shown in Figs. 5 and 7 demonstrate the close correspondence between the salt isopachs and strain in the New York plateau. Moreover, the effects of LPS (integrated value for e_3 ranging from -0.06 to -0.11) are three orders of magnitude larger than the strain due to folding in the middle and upper Devonian section ($e_x = -0.00001$). As there is no evidence of deformation in the pre-Salina section of the New York plateau, the means by which shortening accompanying detachment occurred was almost entirely by differential LPS between the Devonian sequence and the pre-Salina section.

This type of thrust sheet motion is fundamentally different from the two previously recognized mechanisms, imbrication and décollement. As all other mechanisms of sheet motion can be excluded, the thrust tip must move as a zone of LPS in the hangingwall of the thrust sheet. Faults of this type have been suggested by Geiser (1977), Alvarez *et al.* (1978), Coward & Siddans (1979) and Cooper *et al.* (1983). The evidence from the New York plateau seems to represent a clear and unambiguous case that thrusts can form by differential LPS with displacements significant enough to constitute a distinct mechanism for thrust sheet motion.

The following section examines the state of strain in the New York plateau layer-shortening thrust sheet. As described in the previous section, the set of iso-strain contours (Fig. 7) and principal strain trajectories determined from the data in Fig. 5, allow the displacement field to be calculated for the entire plateau. The direction of the displacement field at any point can be found by interpolation between the finite-strain trajectories. The

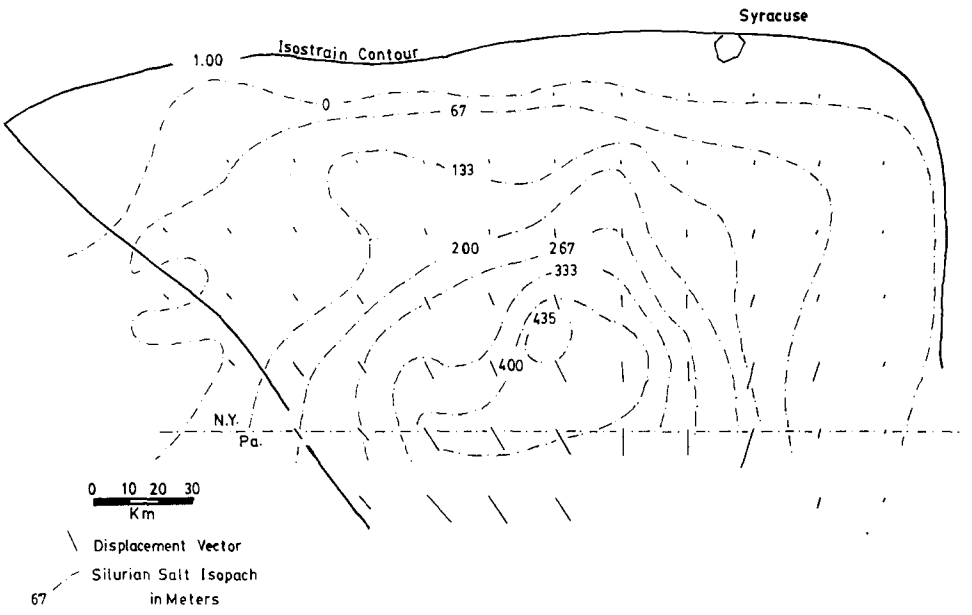

Fig. 10. Displacement field determined from data set given in Fig. 5.

magnitude is given by the difference between the positions of the deformed- and undeformed-state iso-strain contours (see Fig. 8 for example). The displacement field thus calculated (Fig. 10) is used to move the intersection points of the initial orthogonal grids shown in Figs. 11 and 12.

Depending upon the polarity of the displacement used, either a palinspastic reconstruction of the plateau can be made (direction of displacement towards the internides, Fig. 11) or else the present distortion of an initially orthogonal grid can be shown (direction of displacement towards the craton, Fig. 12). These figures show that the southern boundary of the region has been displaced up to 15 km towards the northeast. Significant rotational strain and stretching parallel to strike is indicated in the southeastern part of the plateau (Fig. 12).

The iso-strain contours correlate closely with the salt isopachs, their trend being approximately parallel to the isopachs (Fig. 7). A further correlation exists between the finite strain and the thickness of the salt (Fig. 13). The steepest strain gradients occur along the boundaries of the detachment where the salt thins. However, the relationship between salt thickness and strain is not simple, as the highest strains are found in the eastern part of the sheet near the margin of the basin (if the salt isopachs accurately reflect the basin geometry). At this point the gradient abruptly decreases. To the west finite-strain values remain more or less constant across the thickest part of the salt (although the gradient changes sign), until the western margin of the basin is reached. At this point the gradient increases again, but less radically than it does along the eastern margin. This

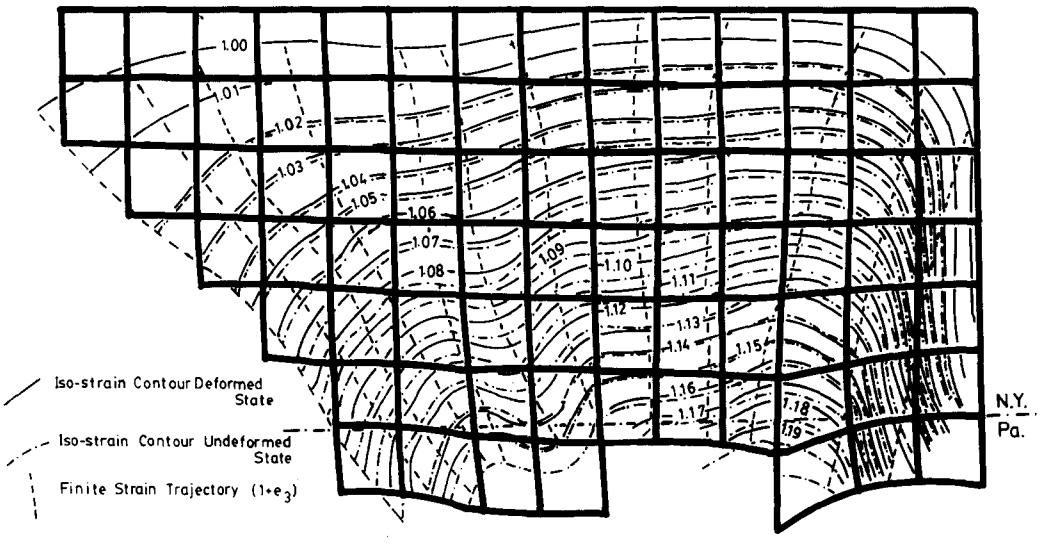

Fig. 11. Palinspastically restored grid constructed using the displacement field shown in Fig. 10 and an initially orthogonal grid in the deformed (i.e. present) state.

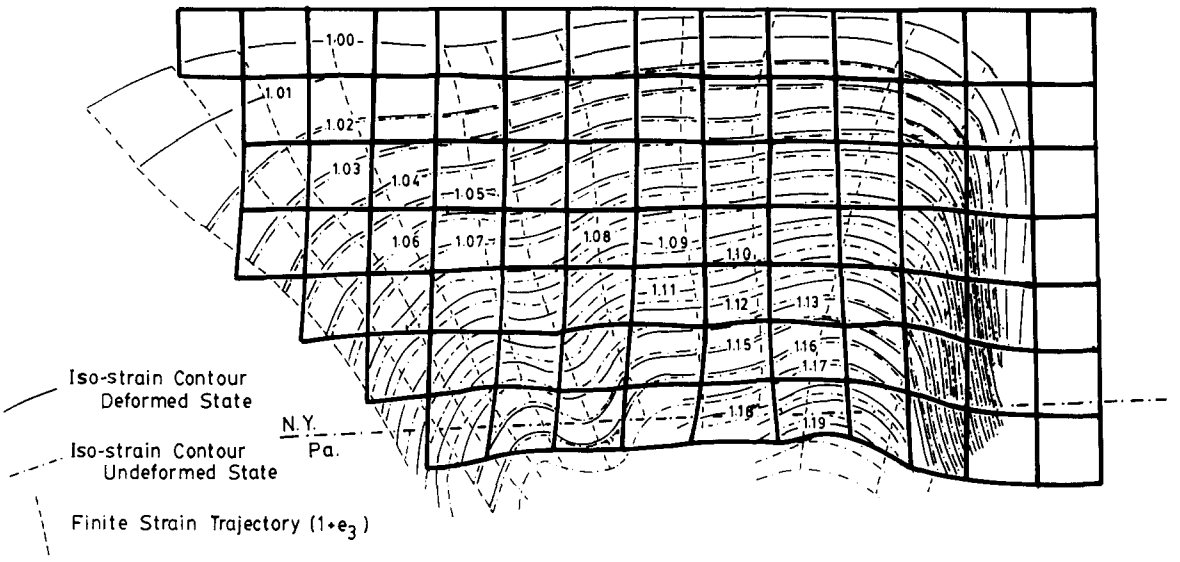

Fig. 12. Deformed grid constructed using the displacement field shown in Fig. 10 and an initially orthogonal grid in the undeformed (i.e. past) state.

lower strain gradient corresponds to the lower salt thickness gradient along the western basin boundary as opposed to the higher strain gradients in the eastern part of the traverse where the salt increases more rapidly in thickness. Again strain variation reflects aspects of stratigraphy and basin geometry.

These observations contrast with those of Elliott (1976a), Mitra (1976, 1978) and Mitra *et al.* (1988), who found a close correlation between LPS fabric development and temperature. These results led Elliott (1976a, p. 310) to suggest that cleavage development, and therefore implicitly LPS, is controlled by temperature. To test this hypothesis I have superposed the CAI isograds (Harris *et al.* 1978) on the iso-strain contours (Fig. 14). The superposition shows no correlation between *LPS strain* and temperature on the New York plateau. A possible connection between cleavage development and temperature is suggested by the cleavage development in the carbonates in the eastern, 'hotter' parts of the plateau. The Tully Limestone shows this particularly well, as it has prominent cleavage from about the middle of the plateau eastwards. Although pressure solution remains the major deformation mechanism (Engelder 1979a,b), cleavage is not found in this unit or any others in the western part of the plateau.

The development of other fabric elements seems unaffected by the variation in temperature. The only exception to this is suggested by the apparent decrease in importance of pressure solution as a deformation mechanism of the crinoid columnals in the eastern part

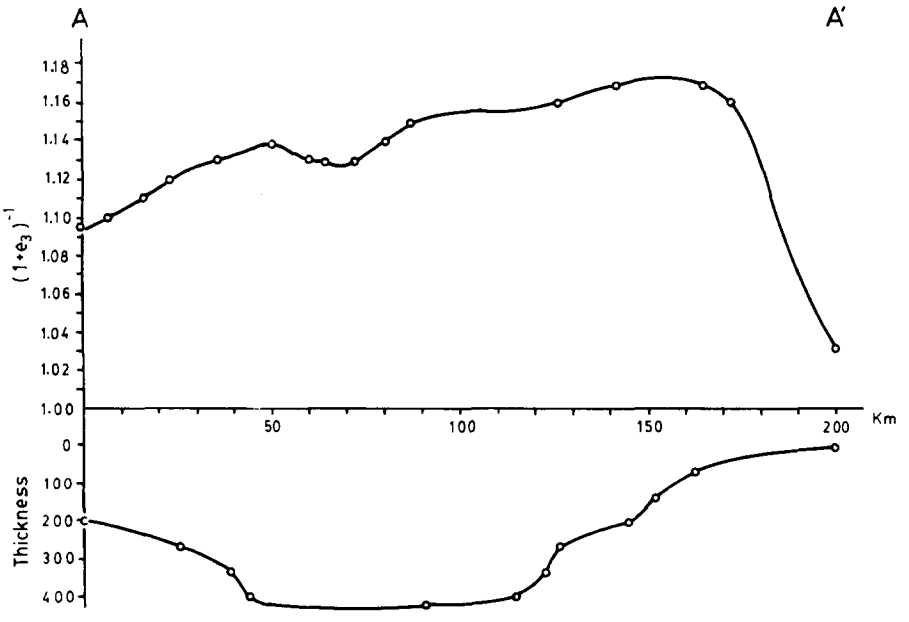

Fig. 13. Plot indicating correspondence between salt thickness (measured in meters) and finite strain along section AA', Fig. 7.

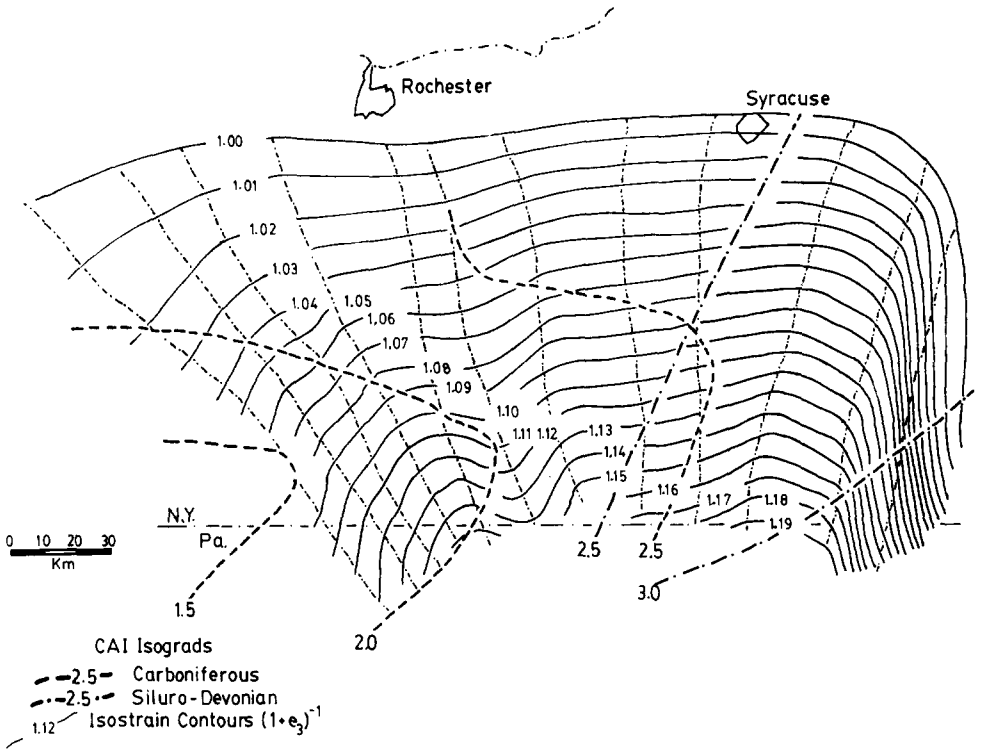

Fig. 14. Map showing lack of correspondence between Conodont Alteration Index (CAI) isograds and layer-parallel shortening strains, New York plateau.

of the plateau. Such an observation would be consistent with the tendency of dislocation–creep mechanisms to dominate at higher temperatures (Elliott 1973, Mitra 1976, 1978). Alternatively, the decrease in importance of pressure solution may be due to a decrease in pore water circulation in more deeply buried parts of the basin (Engelder 1984), or a combination of the two effects.

A final point regards extension of the strain gradient, calculated to be on the order of $\Delta\sqrt{\lambda_x'}/km = +0.0016$ for the eastern New York plateau (Fig. 6a), to the more internal parts of the Appalachians to the south. Such a gradient would result in strains of $\sqrt{\lambda_x} \approx 0.7$ at the Allegheny front, considerably larger than the values of $\sqrt{\lambda_x} = 0.937$ and $\sqrt{\lambda_x} = 0.820$–0.825 found by Faill (1979) and Wright (1982), respectively, for the Valley and Ridge. The implication is that the gradient must level off across the Pennsylvania plateau and possibly even decline. Such a change might correspond to the region of fold amplification near the Allegheny front, where fold limb dips rapidly increase to as much as 20–25°.

HYBRID THRUST SHEETS: SOME EXAMPLES

The three fundamental mechanisms for thrust sheet motion, imbrication, décollement and LPS are not mutually exclusive, but can combine to form various hybrid types when two or more of the end-members operate either simultaneously or sequentially. The structural assemblages created can be described in terms of the three mechanisms. The following outlines some of these hybrid examples and their implications for section construction and interpretation of orogenic history.

In this description a distinction must be made between the stiff layer and the roof layer, as different thrust mechanisms commonly occur in each. The first term of a hybrid refers to the mechanism accommodating the largest proportion of the displacement, while the second or third term gives the other mechanisms in the order of their importance. In the various field examples studied, careful mapping of the strain fabrics generally allows the sequence of the mechanisms to be worked out.

Thrust sheet motion by imbrication and décollement

Thompson (1979) described an example of a thrust sheet from the northern Canadian Cordillera formed by imbricated stiff layer and décollement thrusts in the roof. Displacement on the thick stiff layer of Ordovician to Devonian carbonates, packaged between two shale units, was absorbed by décollement on the higher detachment bounding the forelimb, as well as on the hangingwall flat in front of the forelimb (Fig. 2). Note that kinematics require the displacements on both the horse and the décollement thrust in the roof layer to occur simultaneously. In effect the horse 'inserts' itself into its roof layer by delamination. This characteristic is quite important from the standpoint of balancing the section (see Fig. 4) and is a method for the formation of blind 'passive' or autochthonous roof duplexes (Banks & Warburton 1986, Geiser 1988b).

Two other significant aspects of the geometry are:

(1) The direction of displacement of the décollement in the forelimb is opposite that of the sole thrust and the general direction of tectonic transport. Cutler (1983 personal communication) has suggested that this kinematics can also generate backthrusts, delta structures and pop ups.

(2) Unless delamination occurs, there is no roof thrust in the sense of Boyer & Elliott (1982), as the décollement terminates on the forelimb without creating a fault-bounded package or horse, even though the superficial geometry of the structure is identical to that of a duplex (see for example Boyer & Elliott 1982, fig. 26).

Thrust sheet motion by LPS and décollement

The southern part of the New York plateau, where finite-amplitude folding (Wedel 1932) and LPS are both present, is an example of this type of hybrid thrust system. In this case, however, the sole thrust continues to propagate for over 30 km beyond the region of hybrid thrusting by LPS alone (see fig. 2, Engelder & Geiser 1979). Engelder & Geiser (1979) show that the LPS predates finite-amplitude folding. Thus the hybrid thrust family in the southern part of the New York plateau consists of a set of sequential rather than simultaneously acting thrust mechanisms.

Thrust sheet motion by imbrication–LPS–décollement (Fig. 15)

This type of hybrid sheet was recognized in the central Apennines during mapping by W. Alvarez, T. Engelder, myself and students. Here, the stiff layer, consisting of part of a basal evaporitic sequence (Burrano Formation), grades upwards into a massive reefal limestone (the Massicio Formation) and finally incorporates parts of a series of thin- to medium-bedded dominantly pelagic limestones and cherts (Corniola–Maiolica Formations). Although significant folding does occur in the thinner bedded units above the Massicio, structural sections (e.g. Fig. 15) show that most of the displacement has been absorbed by a combination of intense solution cleavage and folding in the units immediately above the upper detachment in the Marne a Fucoide (i.e. Scaglia Bianca to Scaglia Variagata, Fig. 15). In effect the advancing edge of the hangingwall ramp 'bulldozed' the units above it, producing intense strain, manifest by a combination of folding and solution cleavage. In places the cleavage represents a volume loss of greater than 50% (Alvarez *et al.* 1978). The kinematics are very similar to those described by Thompson (1979), however here the displacement of the hangingwall ramp is accommodated by a simultaneously-operating combination of LPS and décollement rather than décollement alone.

Thrust sheet motion by imbrication and LPS (Fig. 16)

A hybrid thrust sheet, interpreted as consisting of an initial phase of LPS, followed by imbrication, has been recognized on the basis of reconnaissance mapping by myself and more detailed mapping by Marshak (1983, 1985) along the Helderburg Escarpment south of Albany, New York. These relations are spectacularly displayed in a series of road cuts and quarries described by Marshak & Geiser (1980) and Marshak (1983, 1985). A particularly good exposure occurs in the Fuerra Bush quarry near South Bethlehem, New York, where an imbricate fan stacks slices of the Helderberg group containing an earlier cleavage (Fig. 16). Note that in this case it is the stiff layer itself which forms the hybrid thrust. Mapping to the west of the escarpment, in the vicinity of Route 23 (Marshak 1983, 1985), shows that cleavage, the last deformational fabric to disappear, ends about 10 km west, implying that the fault propagated by LPS.

Thrust sheet motion by décollement–imbrication

Another example of a stiff layer hybrid thrust is given by Dahlstrom's (1970, fig. 40) discussion of a 'concentric

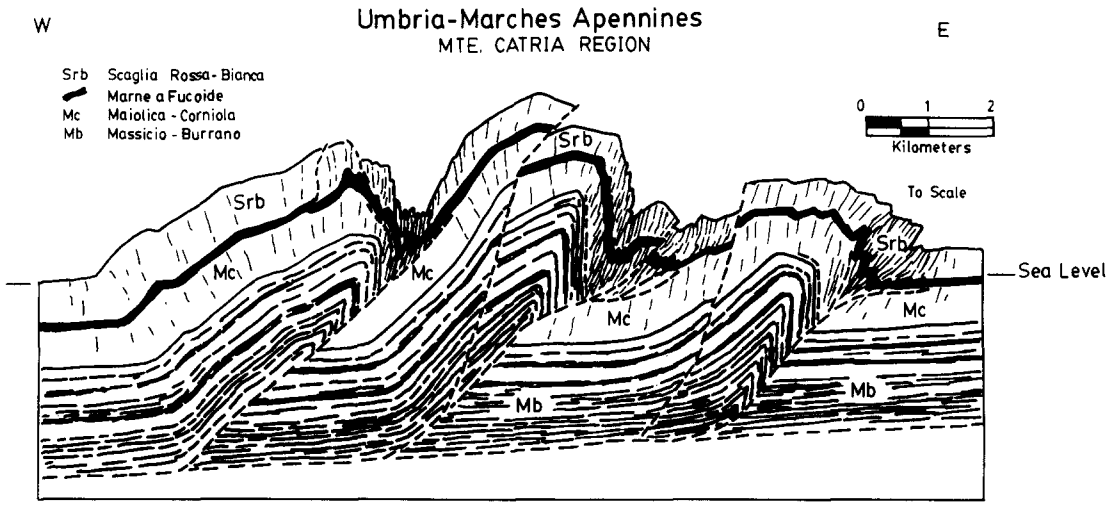

Fig. 15. Profile section of a complex hybrid thrust, central Apennines, Italy. Displacement of roof layer by imbricated stiff layer is absorbed by varying amounts of LPS and décollement thrusting.

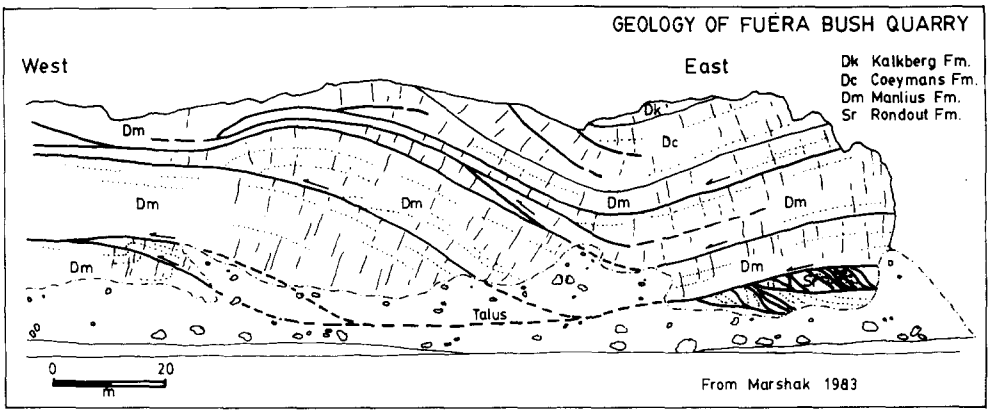

Fig. 16. Profile section of a hybrid thrust at Fuera Bush Quarry, Helderburg Escarpment, Little Mountains, New York. Thrusting was initiated by LPS followed by imbrication. Cleavage is indicated by lines normal to bedding.

fold detachment', in which décollement either precedes or is synchronous with imbrication (Fig. 17). Roeder (1973) describes very similar appearing structures from the Athabasca River profile of the Canadian Rockies, calling them 'frontal zone folds'. Dahlstrom claims this type of structure is one of the most common exposed in the southern Canadian Cordillera and suggests that the initial displacement on the sole thrust is by detachment due to folding. From a kinematic standpoint it is equally possible that the initial displacement was due to imbrication with folding of the stiff layer during subsequent movement.

THE ROLE OF LAYER-PARALLEL SHORTENING IN SECTION BALANCING AND RESTORATION

A major problem in the construction and restoration of geologic sections in blind thrust terranes is bed-length and area balancing (e.g. Gwinn 1970, Perry 1978, Herman 1984). For example, in most sections through the central Appalachians, the roof layer and stiff layer do not balance (Geiser 1988a). This section shows how various hybrid thrusts incorporating LPS may be used to deal with the problem.

The problem occurs in two different types of structures in these regions, duplexes and décollements (Fig. 18a & b). Dahlstrom recognized but did not completely resolve the question of balancing the beds above and below décollements. To resolve the problem of the panel of flat-lying beds above the folded units he posited an *upper* as well as a lower detachment (Dahlstrom 1970, p. 367). In some cases (Dahlstrom 1970, fig. 31) this makes the entire package into a type of ramp, in the sense that the displacement on the sole thrust changes stratigraphic level.

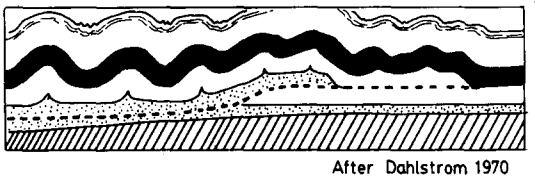

Fig. 17. Schematic section of hybrid décollement–imbricate thrust characteristic of the Southern Canadian Rockies foothills.

There is no need *a priori* for such a detachment, as an alternative solution is readily available in the form of a combination of dip-domain folding (Usdansky & Groshong 1984, Kligfield *et al.* 1986) and LPS in the upper flat-lying units (Fig. 18b). The effect of dip-domain folding is to dissipate displacement continuously rather than discontinously as occurs in concentric folds (also see Faill 1973). Remaining displacement can be accounted for by LPS.

A problem similar to that of Dahlstrom's is encountered in Perry's (1978) sections through the blind thrust terrane of the central Appalachians of West Virginia and Maryland and in Gwinn's (1970) and Herman's (1984) sections through Pennsylvania (Fig. 4). In none of these cases is it possible to achieve either bed-length or area balance beween roof layer and stiff layer. I have chosen Herman's section through the Juniata culmination to illustrate the problem (Fig. 4). As can be seen, the stiff layer is more than 67% longer than the roof layer. Where has the missing roof layer gone? There are several possible answers.

(1) Displacement is absorbed on the Allegheny plateau to the west by some set of deformation mechanisms.

(2) Displacement is absorbed by LPS within the roof layer contained in the section.

(3) Displacement is absorbed by a combination of unspecified mechanisms on the plateau and by LPS within the section shown.

(4) The initial length of the stiff layer was greater than that of the roof layer.

(5) There has been differential lateral flow between the roof layer and the stiff layer, normal to the plane of the section.

The last solution is very difficult to imagine. In any event there is no evidence of significant ($\lambda_y > 1.05$) longitudinal stretching in the central or northern Appalachian roof layer (Engelder & Geiser 1980, Geiser 1988a). A solution that has the displacement of the roof layer absorbed by some combination of décollement and imbrication alone can also be rejected. Numerous struc-

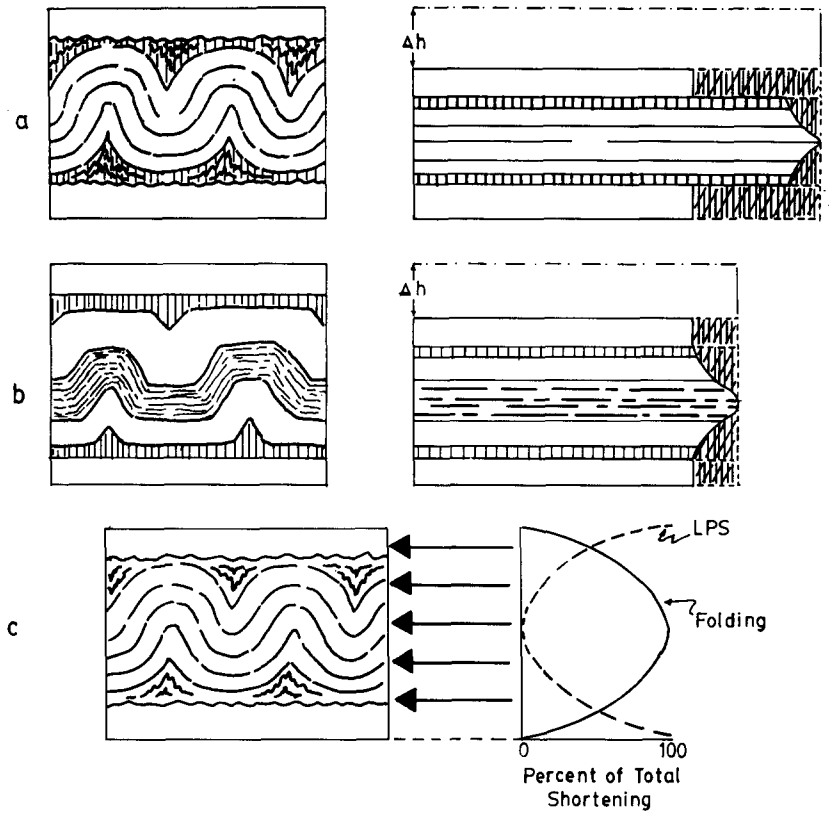

Fig. 18. Contrast in effects on area and bed-length balancing between (a) concentric folds and (b) folds with dip-domain geometry. Cross-hatched region indicates area lost. Δh is the increase in thickness due to folding. It is assumed that bed-length originally balanced in all figures, with the initial length given by the longest bed-length. Deformation is by global pure shear (Geiser 1988b). (c) Partitioning of per cent total shortening between LPS and folding.

tural sections across various parts of the Appalachian plateau demonstrate that no more than about 25 km of the total shortening can be accounted for by décollement and imbrication on the plateau (see for example the state geologic maps of West Virginia and Pennsylvania as well as Gwinn, 1964). In Pennsylvania this amounts to no more than 37% of the displacement which must be absorbed.

Given these arguments, the most likely mechanism to account for the missing roof layer (consisting of all units of essentially Martinsburg age or younger) is LPS. The questions now are: What is the distribution of the LPS? Is there a constant gradient across the entire orogen? Or does it vary in some manner? How is the strain partitioned among the various mechanisms? Again, is there some sort of systematic variation in partitioning? Unfortunately the data to answer these and a host of related questions are available in only the most sketchy form (Geiser 1988a). However it is clear that from the geometric and kinematic role of LPS in absorbing displacement and its widespread distribution in the central and northern Appalachians (Geiser 1988a), that LPS plays a major role in the deformation of this part of the Appalachian orogen and is the most likely mechanism to account for the failure of sections through this region to balance.

I have added the caveat 'likely' to my conclusion, since there is geologic evidence that the stiff layer of Cambro-Ordovician carbonates may have been initially longer than its roof layer (Geiser 1985). However this question cannot be answered without more detailed knowledge of the magnitude and distribution of finite strain in the roof layer rocks of the central and northern Appalachians. Thus, regional finite-strain analysis of the Appalachian foreland, and by implication, other foreland fold-thrust belts as well, seems to hold the key to answering a number of critical questions on the geologic evolution of these terranes.

The presence or absence of LPS in a region can also play a critical role in producing a 'restored' geologic section and in the prediction of the location and amounts of displacement of thrust faults. In the concept of a restored section (Elliott & Johnson 1980), the initial fracture array is used as a type of strain marker. In order that a section be restorable it is necessary that either bed-length and/or area be conserved. In a thrust sheet formed by imbrication and LPS such as that described by Marshak (1983), it is entirely possible that LPS may have involved significant volume loss (e.g. Geiser & Sansone 1981, Wright & Platt 1982). In such a case neither bed-length nor area will be conserved and the section will not be restorable without further information on the nature and distribution of the LPS strain.

A related problem is shown in Fig. 19, in which two geometrically identical cross-sections have two different solutions. In the first (case I) I assume that there is only

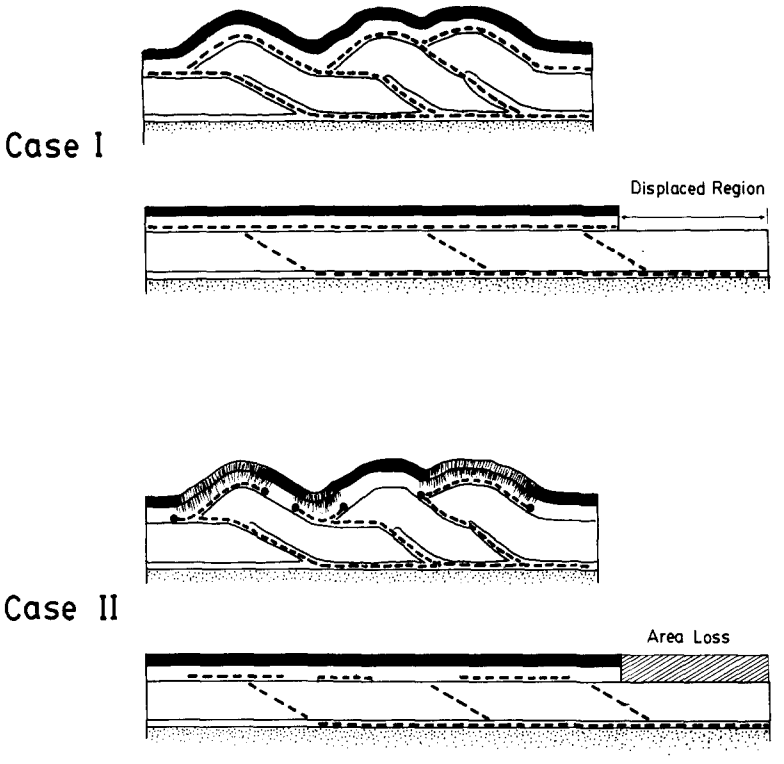

Fig. 19. Schematic diagram illustrating two possible interpretations in blind thrust terranes, utilizing different modes of thrusting. Case I shows an autochthonous roof duplex (Geiser, 1988b) formed by imbrication with displaced roof layer accommodated off-section to the left. This section contains a pin line only for the stiff layer (left-hand boundary). Case II shows an autochthonous roof duplex formed by imbrication with layer shortening thrusts accommodating the missing roof layer. This section contains local pin lines (Woodward *et al.* 1985) at the end of each layer-shortening thrust and a regional pin line at the left-hand boundary.

imbrication forming a duplex. This predicts that (1) a roof thrust is located at the top of the stiff layer; (2) the missing portion of the roof layer represents the amount of displacement which must be accounted for in the adjacent section. In the second (case II) all the roof layer displacement is absorbed by LPS. This predicts that: (1) there is no roof thrust and that parts of the roof layer are pinned to the stiff layer; (2) that the tip of the imbricate thrust occurs in the section and there is no displacement in the adjacent section. It should be noted that both case II (Fig. 19) and Fig. 2 could be mistaken for 'allochthonous roof' (sense of Boyer & Elliott 1982, Geiser 1988b) duplexes when in fact they are blind 'autochthonous roof' duplexes (Geiser 1988b).

Figure 19 illustrates the mechanism for forming a blind 'autochthonous roof' duplex. Although there are similarities in appearance, there are important differences between the structure illustrated in Fig. 19 and that proposed by Banks & Warburton (1986). Banks & Warburton handle the problem of the imbalance between roof layer and stiff layer by eliminating the excess roof layer along a system of emergent thrusts, a model not applicable to the central Appalachians, which lacks emergent faults (Geiser 1988a). To verify which of the two solutions shown in Fig. 19 is the correct one, the areal distribution of any LPS fabric must be found. For the displacement absorbed within the section, it is necessary to actually measure the finite strains associated with the LPS fabric.

A final comment is that if a section fails to balance due to LPS, the strain is either volume-constant or not volume-constant. In the first case the amount of section missing represents the amount of tectonic thickening of the section, thickening which should be reflected in the strain fabric (e.g. down-dip extension in cleavage, large numbers of small contraction faults, etc.). In the second case, the missing section is a measure of volume loss. This redistribution of material should reflect directly on questions of permeability and porosity of the section as well as being evidence of fluid migration. Thus careful analysis of section geometry can shed light on a spectrum of important geological problems in addition to section construction itself.

An important question raised by the scale and behavior of the three mechanisms for thrust sheet motion regards the proposed analogy between the geometry of crystal dislocations and that of thrust faults (Elliott 1976a). While such analogies may be reasonable when the 'ductile bead' is very small compared to the size of the thrust surface, it seems a questionable procedure to blindly extend this analogy to faults where the 'ductile bead' is a significant fraction of the size of the thrust sheet, or is in fact the entire thrust sheet. In any event Elliott's original usage was applied to the geometry of imbrication only, its relation to other types of deformation mechanisms has not been studied. Given the limited knowledge of the geometry and relations between the three mechanisms, it would seem prudent to utilize

considerable caution in applying the crystal dislocation analogy.

In summary, it is felt that the existence of three interactive mechanisms of thrust sheet motion raises new questions about out understanding of the geometry of thrust faults and their propagation, questions which relate to our understanding of thrust belt mechanics. Answering these questions requires systematic study of all three mechanisms to thoroughly document the interactions among the three types. Thus regional finite-strain analysis of the type pioneered by Ernst Cloos (1947, 1971) and the construction of physically-possible geological cross-sections, must become a routine part of the geological investigation of foreland overthrust terrane. Without these data our understanding of overthrust belts will be hampered and answers to problems of accurate palinspastic reconstructions, plate interactions and the mechanics of orogenesis will continue to elude us.

CONCLUSIONS

I have presented evidence that there exist three fundamental mechanisms for thrust motion and tip propagation: imbrication, décollement and LPS. The mechanisms may work either independently or interactively to distribute the displacements involved in the formation of overthrust terranes. Thus in addition to the 'pure' thrust sheets, various 'hybrids' consisting of two or more mechanisms can arise. As pointed out by J. Cutler (1983, personal communication), this behavior may effectively be a type of thrust partitioning among the various components of a strain decomposition, with imbrication = 'rigid-body' translation, LPS = pure strain and décollement = rotation.

As a part of this analysis, data from the New York plateau provide the first documentation demonstrating that LPS can act as the dominant mechanism for the accommodation of thrust sheet motion. The data show that:

(1) LPS is of regional extent and has allowed for displacements of parts of the sheet by a minimum of 15 km;

(2) displacements associated with LPS are three orders of magnitude larger than those due to all other types of deformation in this same region;

(3) strain gradients associated with the thrust correlate with thickness gradients in the salt detachment horizon, changing as thickness changes and remaining constant where thickness is constant;

(4) variation in finite LPS strain is shown to be independent of temperature and depth of burial, but to correlate with thickness changes in the salt and thus is inferred to reflect variation in the surface geometry of the sole fault;

(5) the areal extent of the thrust sheet can be determined by mapping the extent of LPS fabrics and associated finite strains. A method is also presented showing how to create iso-strain maps in both the deformed and undeformed states from the finite-strain data. These maps are used to determine the displacement field for the thrust sheet. The displacement field is in turn utilized to show its effects on an initially orthogonal grid in both the deformed (i.e. present) and undeformed (i.e. palinspastically restored) states.

The three mechanisms occur in all mountain belts. LPS is regionally developed throughout the central and northern Appalachians and can account for much of the missing section in this and perhaps in other thrust terranes. The 'imbalance' itself is useful information as it has a direct bearing not only on the finite strain and kinematics, but also on aspects of the fluid migration history and the porosity and permeability of the stratigraphic column.

Acknowledgements—Important contributions to this work were made by Terry Engelder, Walter Alvarez, James Slaughter and Greg Herman, while discussions with Norman Gray and James Geiser added much to its quality. Field assistance from Gail Moritz and Kathy Brockett in the Appalachians and from Alessandro Montenari, Mark Rowan and Kevin Stuart in the Apennines are gratefully acknowledged. Critical readings of versions of this paper by Dave Gray, Terry Engelder, Jon Cutler, Rick Groshong, Fred Diegel and an anonymous reviewer helped materially to improve the manuscript. Funding was provided by National Science Foundation grants EAR 77-14431, EAR 79-11085, EAR 82-07355 and the University of Connecticut Research Foundation.

REFERENCES

Alvarez, W., Engelder, T. & Geiser, P. A. 1978. Classification of solution cleavage in pelagic limestones. *Geology* **6**, 263–266.

Banks, C. J. & Warburton J. 1986. 'Passive-roof' duplex geometry in the frontal structures of the Kirthar and Sulaiman mountain belts, Pakistan. *J. Struct. Geol.* **8**, 229–238.

Boyer, S. E. & Elliott, D. 1982. Thrust systems. *Am. Ass. Petrol. Geol.* **66**, 1196–1230.

Cloos, E. 1947. Oolite deformation in South Mountain fold, Maryland. *Bull. geol. Soc. Am.* **58**, 843–918.

Cloos, E. 1971. *Microtectonics along the Western Edge of the Blue Ridge, Maryland and Virginia.* Johns Hopkins University Press, Baltimore, Maryland.

Cooper, M. A., Garton, M. R. & Hossack, J. R. 1983. The origin of the Basse Normandie duplex, Boulonnais, France. *J. Struct. Geol.* **5**, 139–152.

Coward, M. P. & Siddans, A. W. B. 1979. The tectonic evolution of the Welsh Caledonides, in the Caledonides of the British Isles—Reviewed. *J. geol. Soc. Lond.* **136**, 187–198.

Cutler, J. & Elliott, D. 1983. The compatibility equations and the pole to the Mohr circle. *J. Struct. Geol.* **5**, 287–298.

Dahlstrom, C. D. A., 1970. Structural geology in the eastern margin of the Canadian Rocky Mountains. *Bull. Can. Petrol. Geol.* **18**, 332–406.

Elliott, D. 1973. Diffusion flow laws in metamorphic rocks. *Bull. geol. Soc. Am.* **84**, 2645–2664.

Elliott, D. 1976a. The energy balance and deformation mechanisms of thrust sheets. *Phil. Trans. R. Soc.* **A273**, 289–312.

Elliott, D. 1976b. The motion of thrust sheets. *J. geophys. Res.* **81**, 949–963.

Elliott, D. & Johnson, M. R. W. 1980. Structural evolution in the northern part of the Moine thrust belt, NW Scotland. *Trans. R. Soc. Edinb., Earth Sci.* **71**, 69–96.

Engelder, T. 1979a. Mechanisms for strain within the upper Devonian clastic sequence of the Appalachian Plateau, western New York. *Am. J. Sci.* **279**, 527–542.

Engelder, T. 1979b. The nature of deformation within the outer limits of the central Appalachian foreland fold and thrust belt in New York State. *Tectonophysics* **55**, 289–310.

Engelder, T. 1984. The role of pore water circulation during the deformation of foreland fold and thrust belts. *J. geophys. Res.* **89**, 4319–4325.

Engelder, T. & Engelder, R. 1977. Fossil distortion and décollement

tectonics on the Appalachian Plateau, New York. *Geology* **5**, 457–460.
Engelder, T. & Geiser, P. 1979. The relationship between pencil cleavage and lateral shortening within the Devonian section of the Appalachian Plateau, New York. *Geology* **7**, 460–464.
Engelder, T. & Geiser, P. 1980. On the use of regional joint sets as trajectories of paleostress fields during the development of the Appalachian Plateau. *J. geophys. Res.* **85**, 6319–6341.
Faill, R. T. 1973. Kink band folding, Valley and Ridge province, Pennsylvania. *Bull. geol. Soc. Am.* **84**, 1289–1314.
Faill, R. T. 1979. Geology and mineral resources of the Mountoursville South and Muncy quadrangles and part of the Hughsville quadrangle, Lycoming, Northumberland and Montour counties Pennsylvania. Commonwealth of Pennsylvania, Dept. of Env. Resources, Bur. Topographic and Geol. Survey, Atlas 144ab.
Faill, R. T. & Nickelsen, R. P. 1973. Structural geology. In: *38th Annual Field Conf. of Pennsylvania Geologists* (edited by Faill, R. T.), 9–38.
Geiser, P. A. 1970. Deformation of the Bloomsburg formation, Cacapon Mountain Anticline, Maryland. Unpublished Ph.D. thesis, Johns Hopkins University, Baltimore, Maryland.
Geiser, P. A. 1974. Cleavage in some sedimentary rocks of the Valley and Ridge province, Maryland. *Bull. geol. Soc. Am.* **85**, 1399–1412.
Geiser, P. A. 1977. Early deformation structures in the central Appalachians: a model and its implications. *Geol. Soc. Am. Abs. w. Prog., N.E. Section* **7**.
Geiser, P. A., 1985. Evidence for Taconic age deformation of the Central Appalachian foreland. *Geol. Soc. Am. Abs. w. Prog.*, N.E. Section **15**.
Geiser, P. A. 1988a. The central Appalachian foreland of the Alleghanian orogen. In: *The Appalachian Orogen, DNAG Volume* (edited by Hatcher, R. D. & Thomas, W. M.), *Geol. Soc. Am.*, in press.
Geiser, P. A. 1988b. The role of kinematics in the construction and anlaysis of geological cross sections in deformed terranes. In: *Geometry and Mechanisms of Faulting with Special Reference to the Appalachians* (edited by Mitra, G. & Wojtal, S.). *Spec. Pap. geol. Soc. Am.* **222**, in press.
Geiser, P. A. & Engelder, T. 1983. The distribution of layer parallel shortening fabrics in the Appalachian foreland of New York and Pennsylvania: evidence for two non-coaxial phases of the Alleghanian orogeny. In: *Mem. geol. Soc. Am.* (edited by Hatcher, R. D., Williams H. & Zeitz, I.), **158**, 161–175.
Geiser, P. A. & Sansone, S. 1981. Joints, microfractures, and the formation of solution cleavage in limestone. *Geology* **9**, 280–285.
Gwinn, V. E. 1964. Thin skinned tectonics in the plateau and northwestern Valley and Ridge provinces of the central Appalachians. *Bull. geol. Soc. Am.* **75**, 863–900.
Gwinn, V. E. 1970. Kinematic patterns and estimates of lateral shortening, Valley and Ridge and Great Valley provinces, central Appalachians, south central Pennsylvania. In: *Studies of Appalachian Geololgy: Central and Southern* (Cloos Volume) (edited by Fisher, G. W., Pettijohn, F. J., Reed, J. C. & Weaver, K. N.). J. Wiley & Sons, New York, 127–146.
Harris, A. G., Harris, L. D. & Epstein, J. B. 1978. Oil and gas data from Paleozoic rocks in the Appalachian basin: Maps for assessing hydrocarbon potential and thermal maturity (Conodont color Alteration Isograds and overburden isopachs). Dept of the Interior, U.S.geol. Surv., Misc. Invest. Ser. Map I-917-E.
Herman, G. C. 1984. A structural analysis of a portion of the Valley and Ridge province of Pennsylvania. Unpublished MS. thesis, University of Connecticut.
Hobbs, B. E., Means, W. D. & Williams, P. F. 1976. *An Outline of Structural Geology*. John Wiley & Sons, New York.
Hossack, J. R. 1978. The correction of stratigraphic sections for tectonic finite strain in the Bygdin area, Norway. *J. geol. Soc. Lond.* **135**, 229–241.
Kligfield, R., Geiser, P. A. & Geiser, J. R. 1986. *Construction of Geologic Cross-Sections Using Microcomputer Systems*. Geobyte, Springer, New York, 60–66.
Kulander, B. R. & Dean, S. L. 1986. Structure and tectonics of central and southern Appalachian Valley and Ridge and Plateau provinces, West Virginia and Virginia. *Bull. Am. Ass. Petrol. Geol.* **70**, 1674–1684.
Laubscher, H. P. 1961. Die fernschubhypothese der Jura faltung. *Eclog. geol. Helv.* **54**, 221–282.
Marshak, S. 1983. Aspects of deformation in carbonate rocks of fold-thrust belts of central Italy and eastern New York state. Unpublished PhD. thesis, Columbia University.
Marshak, S. 1985. Structure and tectonics of the Hudson Valley fold-thrust belt, New York. *Bull. geol. Soc. Am.* **97**, 354–368.
Marshak, S. & Geiser, P. A. 1980. Guidebook to pressure solution phenomena in the Hudson Valley. *Field excursion—GSA Penrose Conference, the Role of Pressure Solution and Dissolution Phenomena in Geology: An Interdisciplinary Conference.*
Marshak, S., Geiser, P. A., Alvarez, W. & Engelder, T. 1982. Mesoscopic fault array of the northern Umbrian Apennine fold belt, Italy: geometry of conjugate shear by pressure solution slip. *Bull. geol. Soc. Am.* **93**, 1013–1022.
Mitra, S. 1976. A quantitative study of deformation mechanisms and finite strain in quartzites. *Contr. Miner. Petrol.* **59**, 203–226.
Mitra, S. 1978. Microscopic deformation mechanisms and flow laws in quartzites within the South Mountain anticline. *J. Geol.* **86**, 129–152.
Mitra, G., Hull, J. M., Yonkee, W. A. & Protzman, G. M. 1988. Comparison of meso and microscale deformational styles in the Idaho–Wyoming thrust belt and Rocky Mountain foreland. In: *Interaction of Rocky Mountain Foreland and Cordilleran Thrust Belt* (edited by Perry, W. J. & Schmidt, C. J.). *Spec. Pap. geol. Soc. Am.*, in press.
Nickelsen, R. P. 1966. Fossil distortion and penetrative rock deformation in the Appalachian plateau, Pennsylvania. *J. Geol.* **74**, 924–931.
Perry, W. J. Jr. 1978. Sequential deformation in the central Appalachians. *Am. J. Sci.* **278**, 518–542.
Ramsay, J. G. 1967. *Folding and Fracturing of Rocks*. McGraw-Hill, New York.
Ramsay, J. G. 1969. The measurement of strain and displacement in orogenic belts. In: *Time and Place in Orogeny* (edited by Kent, P. E., Satterwaite, G. E. & Spencer, A. M.). *Spec. Publs geol. Soc. Lond.* **3**, 43–80.
Ramsay, J. G. & Huber, M. I. 1983. *The Techniques of Modern Structural Geology. Volume* 1: *Strain Analysis*. Academic Press, New York.
Rich, J. L. 1934. Mechanics of low-angle overthrust faulting as illustrated by Cumberland thrust block, Virginia, Kentucky and Tennessee. *Bull. Am. Ass. Petrol. Geol.* **33**, 1643–1654.
Rodgers, J. 1970. *The Tectonics of the Appalachians*. John Wiley & Sons, New York.
Roeder, D. 1973. Subduction and orogeny. *J. geophys. Res.* **78**, 5005–5024.
Shimamoto, T. & Ikeda, Y. 1976. Simple algebraic method for strain estimation from deformed ellipsoidal objects, 1. Basic theory. *Tectonophysics* **36**, 315–337.
Slaughter, J. A. 1982. Fossil distortion and pressure solution in the middle to upper Devonian clastics and limestones of the Appalachian Plateau, central New York. Unpublished M.S. thesis, University of Connecticut.
Suppe, J. 1983. Geometry and kinematics of fault bend folding. *Am. J. Sci.* **283**, 684–721.
Thompson, R. I. 1979. A structural interpretation across part of the northern Rocky Mountains British Columbia, Canada. *Can. J. Earth Sci.* **16**, 1228–1241.
Usdansky, S. & Groshong, R. 1984. Comparison of analytical models for dip-domain and fault bend folding (abs.). *Geol. Soc. Am. Abs. w. Prog.* **16**, 680.
Wedel, A. A. 1932. Geologic structure of the Devonian strata of south central New York. *N.Y. state Mus. Bull.* **294**, 74.
Wiltschko, D. V. & Chapple, W. M. 1977. Flow of weak rocks in Appalachian plateau folds. *Bull. Am. Ass. Petrol. Geol.* **61**, 653–670.
Woodward, N. B., Boyer, S. E. & Suppe, J. 1985. *An Outline of Balanced Sections*, 2nd edn. University of Tennessee, Dept of Geological Sciences. *Studies in Geology* **11**.
Wright, T. O. & Platt, L. B. 1982. Pressure dissolution and cleavage in the Martinsburg Shale. *Am. J. Sci.* **282**, 122–135.